SCIREA Journal of Materials

http://www.scirea.org/journal/Materials

April 23, 2018

Volume 3, Issue 2, April 2018

Low Density Polyethylene-Activated Carbon Composite Foams: Preparation and Properties

Darunee Aussawasathien*[a], Kotchaporn Jariyakun[b], Thongchai Pomrawan[b], Kittipong Hrimchum[a], Rungsima Yeetsorn[b], and Walaiporn Prissanaroon-Ouajai [b]

[a]Plastics Technology Lab, Polymer Research Unit, National Metal and Materials Technology Center, Pathumthani 12120, Thailand

[b]Department of Industrial Chemistry, King Mongkut's University of Technology North Bangkok, 1518 Pracharat 1 Road, Wongsawang, Bangsue, Bangkok 10800, Thailand

*Author for correspondence; e-mail: daruneea@mtec.or.th

ABSTRACT

Low density polyethylene (LDPE) containing activated carbon (AC) was foamed with azodicarbonamide (ADC) through an extrusion process. The effects of ADC and AC contents on the cellular structure, void fraction, density, thermal and mechanical properties, and crystallinity of composite foams were investigated. The density of composite foams decreased but the void fraction increased when the ADC content increased. At low AC dosages, the density decreased with increasing void

fraction compared to composite foams without AC. Cell formation and average cell density decreased with increasing AC concentration. The maximum reduction of density by 30% with void fraction of 30% was achieved when ADC and AC were applied at 7 wt% and 10 wt% respectively. Increasing ADC and AC contents resulted in composite foams with lower tensile and impact strengths. The crystalline temperature (T_c) and melting temperature (T_m) changes were insignificant as the ADC and AC loadings increased. The decomposition temperature (T_d) tended lower as the ADC loading increased, whereas an increase in AC content resulted in increasing T_d of the composite foams. The crystallinity percentage of the composite foams reduced slightly with increasing ADC content, but sharply decreased with the enhancement of AC loading.

Keywords: Low density polyethylene; Activated carbon; Azodicarbonamide; Composite foam

1. INTRODUCTION

Foaming technology is a well-known process to produce light-weight materials with a significant expansion ratio, high porosity, and weight reduction. Foam materials have a number of applications such as insulation, surface protection, cushioning due to their high surface area, high permeability, light weight, and low thermal conductivity. They can be manufactured through various foaming techniques e.g. injection molding, compression molding, and extrusion processes [1-3]. The extrusion method has been extensively utilized for making low-density foam sheet based on polystyrene, polypropylene, and polyethylene as examples, using a physical foaming agent (PFA) or chemical foaming agent (CFA) [3-5]. The CFA is mixed directly with the thermoplastic and additives/ fillers before the foaming process, while the PFA needs additional devices for injecting the gases into the machines. CFAs are usually classified into two groups as exothermic and endothermic foaming

agents, providing different effects on morphology, distribution, and cell size. Bledzki and Faruk demonstrated that exothermic CFAs were more effective than endothermic ones in decreasing density and increasing tensile strength of the material [6]. Various CFAs have been used to make polymeric foams. ADC has the most widespread usage owing to its high gas yield and also the possibility of adjusting its decomposition temperature to be compatible with the polymer processing temperature through the use of suitable activators, for example, zinc oxide (ZnO) [7, 8]. The gases released by ADC are mainly nitrogen and carbon monoxide. The basic foaming process consists of three major mechanisms: cell nucleation, cell growth, and cell coalescence. By selecting foaming materials and foaming processes, the formation of open or closed cells can be controlled. In closed cell foams, each cellular structure is surrounded by a complete cell wall and all cells are separated. In open cell foams, all cells are virtually connected to each other in the absence of the cell walls. The proper distribution of the CFA in the polymer matrix generates a uniform fine-celled or microcellular structure, demonstrated as extremely effective in improving the mechanical properties of polymeric foams [9, 10].

The mixture of functional fillers and polymers has created a new class of materials known as polymer composite foams. These materials possess enhanced properties and specific performances as a consequence of the multifunctional role played by the fillers in such systems. Fillers act as nucleating agents for bubble formation, which simultaneously influence the cell morphology and overall macroscopic properties of polymer composite foams [4, 11]. A variety of polymers such as polypropylene, polylactic acid, polystyrene, polyurethane, polycarbonate, poly-methyl-methacrylate, and polyethylene mixed with several types of filler particles such as nanoclays, carbon nanotubes, carbon nanofibers or silica particles [3, 4, 8, 12, 13] have recently been investigated. LDPE does not have an adequate crystallinity to warrant a fast solidification to sustain thin cell walls, however, its branching nature makes it unique in maintaining enough stretching strength to allow continuous extrusion of low density foam sheet. AC is a highly porous material and extensively used to remove a variety of pollutants such as dyes, heavy metals, pesticides, and gases due to its large

specific surface area and high adsorption capacity [14, 15]. It is useful in many industrial sectors such as food, pharmaceutical, chemical, oil, mining and in the treatment of both waste and drinking water [16].

In this study, the polymer composite foams based on LDPE and AC were prepared through the sheet extrusion method. The effects of ADC and AC on cell morphology, density, void fraction, and the physical and mechanical properties were determined.

2. EXPERIMENTAL PROCEDURE

2.1 Materials

LDPE (LD2426K) supplied by PTT Polymer Marketing Co., Ltd., Thailand was used as a base material. Its melt flow index (MFI) was 4 g (10 min)$^{-1}$ at 190^{o}C and 2.16 kg and its density was 0.924 g cm^{-3} at room temperature. AC (CGC-11A 200C) was purchased from Gigantic Carbon Co., Ltd., Thailand, with surface area and average particle size of 1000-1100 m^2 g^{-1} (N_2 BET method) and 74 μm, respectively. ADC (Sunfoam SB00P, exothermic foaming agent with particle size ranging from 8 to 11 μm) supplied by Lautan Luas (Thailand) Co., Ltd., Thailand was used to achieve the microcellular structure in the polymer composite foams. ZnO (99% purity, industrial grade, Thai-Lysaght Co., Ltd., Thailand), and Anox 20 (Optimal Tech Co., Ltd., Thailand) were utilized as the ADC activator and primary antioxidant, respectively.

2.2 Compounding and fabrication

The composition of LDPE-AC composite foams is presented in Table 1. Mixtures of all the materials were premixed in a blending machine at 500 rpm for 10 min, and then compounded by a melt mixing process in a twin screw extruder (LTE20-32, Labtech Engineering Co., Ltd., Thailand). The screw diameter, screw length, and screw L/D ratio were 20 mm, 64 cm, and 32, respectively. The set-up temperature of

the mixing screws was in the range of 130-165°C. The rotation speeds of feeding screws and mixing screws were 12 and 140 rpm, respectively. The extrudate was cooled in a water bath and subsequently granulated using a pelletizer. Composite foam sheets were prepared by a single screw extruder (HAAKE Rheomex driver7, L/D ratio of 25, LMS Instruments Co., Ltd., Thailand) at 220°C (decomposition temperature of ADC is approximately 201-205°C), with a screw speed of 240 rpm. The composite foam sheets were passed through rollers with rolling speed of 35 rpm at 30°C and rolled up for further characterization.

2.3 Characterization methods

The apparent densities of both foamed and un-foamed composites size 1 cm × 1 cm were determined by helium (He) gas displacement technique using an automatic gas pycnometer (Ultrapyc 1200e, Science Engineering and Service Co., Ltd., Thailand) at 17.0 psi and 30°C. The void fraction (V_f) of the foams was determined by Eq. (1) from the densities of neat LDPE sheet (ρ_p) and the composite foam (ρ_f).

$$V_f = 100 \text{ x } \left[1 - \frac{\rho_f}{\rho_p} \right] \qquad (1)$$

The cellular structure of LDPE-AC composite foams was characterized by a Schottky field-emission scanning electron microscope (SEM, SU5000, Coax Group Corp. Ltd., Thailand). Samples were freeze-fractured in liquid nitrogen and the fractured surface was made conductive by sputtering deposition of a thin layer of platinum. The dispersion degree of AC particles in the composite foams was also determined. Cell size and cell density were measured using an image processing tool based on the software ImageJ [17]. The cell population densities per unit area of composite foams were determined from the SEM micrographs using Eq. (2).

$$\text{Cell density} = \left[\frac{n}{A} \right] \frac{3}{2} \text{x} \left[\frac{\rho_f}{\rho_p} \right] \qquad (2)$$

where A is the area of the micrograph (cm^2), n is the number of bubbles in the SEM micrograph, ρ_p is the density of neat LDPE sheet, and ρ_f is the density of the composite foam.

The T_m and the degree of crystallinity (X_c) of neat LDPE and LDPE-AC composite foams were determined using differential scanning calorimetry (DSC, DSC1, Mettler Toledo (Thailand) Ltd., Thailand) under nitrogen atmosphere, while heating the samples from 0 to 170°C at a rate of 20°C min^{-1}. The X_c was calculated from the measurements of the melting enthalpy of 100% crystalline LDPE (ΔH_m = 293.6 J g^{-1}) and the crystallization enthalpies (ΔH_c) as shown in Eq. (3).

$$Xc \quad (\%) \quad = \quad \frac{\Delta\, Hc}{\Delta\, Hm} x\,100 \qquad (3)$$

The effect of ADC and AC concentrations on the thermal stability of both foamed and non-foamed composites was evaluated by thermogravimetric analysis (TGA, SDTA851^e, Mettler Toledo (Thailand) Ltd., Thailand). Samples were heated from 30 to 700°C at a heating rate of 20°C min^{-1} under nitrogen atmosphere. The thermal stability of the samples was determined using the peak of the first derivative curve of the thermograms. The amount of samples used for each DSC and TGA run was approximately 7-10 mg.

The impact strength of the specimens was tested using an impact tester (ITR2000, Intro Enterprices Co., Ltd., Thailand**)** following ASTM D6110. The sheet sample size 5 cm × 5 cm × 0.1 cm was placed on the sample holder and a testing ball was dropped onto the sample with a speed of 3.46 m s^{-1}. The tensile properties were determined according to ASTM D638 using a universal testing machine (55R4502, Instron (Thailand) Co., Ltd., Thailand), equipped with a 10 kN capacity load cell with a crosshead speed of 50 mm min^{-1}. The specimen dimensions were 60 mm × 6 mm × 1 mm. The tensile strength and elongation at break were determined from load-displacement curves. The samples were collected from extruded parts, parallel and transverse to the extrusion direction, and conditioned for at least 3 days at room

temperature. The reported results of the impact and tensile tests were averaged values from ten sample measurements.

3. RESULTS AND DISCUSSION

3.1 SEM micrographs

Figures 1 and 2 show SEM micrographs of composite foams with different ADC and AC dosages respectively. All examples were closed cell and the cell size and cell size distribution were influenced by the different amounts of ADC and AC. The cell feature of composite foams showed irregular holes with various sizes. This morphology suggested a potential incidence of cell collapse due to the low melt strength of LDPE during compounding. Furthermore, composite foams mostly presented unsymmetrical oval shapes, because of the compressive forces generated between the two rollers in the sheet casting process during sample collection. The average cell sizes of the composite foams were in the range of 30-150 μm. The cell density of the composite foams increased from 1.3×10^3 to 1.1×10^6 cells cm^{-2} as the ADC concentration increased (see Figure 3 (a)), because a higher ADC concentration produced more gas from the thermal degradation of the foaming agent [18]. An increase in porous structures was observed in the composite foams containing higher amounts of ADC. As shown in Figure 3 (b), the cell density increased from 8.7×10^5 to 1.3×10^6 cells cm^{-2} when the amount of AC increased from 0 to 10 wt% and then decreased to 1.2×10^6 and 1.1×10^6 cells cm^{-2} for composite foams containing 15 and 20 wt% of AC respectively. The addition of AC up to 20 wt% decreased the cell formation and minimized the cell size. Although the AC particles assisted in generating more foaming nucleation sites in the polymer matrix, high AC agglomeration was created with large amounts of AC which enhanced the resistance against cell growth and produced cells with smaller sizes [19]. Moreover, the specimens with high AC content showed ACs as partially agglomerated which were indicated by arrow signs in Figure 2 (a-2)-(e-2), resulting in the mitigation of the nucleating effect of the particles. A high degree of particle dispersion can lead to a

high nucleating efficiency, whereas a high content of particle agglomeration can decrease the effectiveness of particles as bubble nucleating agents [4, 11]. The AC aggregates indicated that the shear forces produced during the melt mixing step might be inadequate to achieve complete dispersion of the AC particles.

3.2 Density and void fraction

Figures 4 (a) and (b) present the density and void fraction of LDPE-AC composite foams at different ADC and AC concentrations respectively. The composite foams showed a reduction of density from 0.9104 to 0.6649 g cm^{-3} with increasing ADC content from 0 to 7 wt% at 5 wt% AC concentration, because the amount of liberated gas was proportional to ADC content. It is commonly believed that high amounts of released gas generate many cells in the composite foam, resulting in a high degree of void fraction (~ 23-28%). The density of composite foams decreased from 0.6686 to 0.6411 g cm^{-3}, whereas the void fraction increased from 27 to 30% as the AC dosage increased from 0 to 10 wt%, since more foaming nucleation centers were induced by adding AC into the composite foam leading to more gas bubble creation and further cell growth [20]. However, the density of composite foams tended to increase to 0.6551 and 0.7230 g cm^{-3} with the decrease of void fraction from 29 to 21% at AC contents of 15 and 20 wt% respectively, corresponding to the SEM results. The void fraction reduced with increasing AC content since LDPE resin in the composite foam acted as a gas bubble growing site. Therefore, a decrease in resin content could lead to reduced cell quantities in the composites [21].

3.3 Tensile strength and elongation at break

The tensile strength at yield and elongation at break in machine and transverse directions of composite foams containing different amounts of ADC and AC are presented in Figures 5 (a) and (b), and Figures 6 (a) and (b) respectively. The tensile strength and elongation at break of composite foams decreased from 8 to 4 MPa, and

from 35 to 15%, respectively with an increase in ADC from 0 to 7 wt% at 5 wt% AC loading. It was observed that lower density was associated with lower tensile properties, since the presence of voids in the polymer matrix introduced inhomogeneous structures decreasing the ability to transfer stresses. Blair et al. showed that increase in cell size related to decrease in density, and the tensile and comparative strengths of the composite were reduced [22]. Moreover, the tensile properties of composite foams containing AC drastically decreased compared with LDPE resin due to the high stiffness of AC particles, the irregular cellular structure of composite foams, and the reduction of LDPE content. The AC in the solid phase of the foaming process could not be foamed and the gas could not be solved in AC particles [9]. Therefore, the solubility was limited to the polymer. Furthermore, a proper connection between the polymer and AC was not generated at the interface due to bubble formation which prevented the suitable transfer of stresses. By adding AC in composite foams from 0 to 20 wt% at 7 wt% ADC content, the composite tensile strength and elongation at break slightly decreased from 5.8 to 4.0 MPa, and from 38 to 20% respectively. At high AC contents, a significant reduction in strength and elasticity modulus occurred probably due to the formation of AC agglomeration, especially with increase in AC up to 20 wt%, including the presence of voids and low LDPE content. These agglomerates acted as defects in the composite, which could induce an untimely failure when the interfacial adhesion to the surrounding matrix was poor [23].

3.4 Impact Strength

Figures 7 (a) and (b) show the impact strength of the composites with different amounts of ADC and AC respectively. Impact resistance shows the strength of the material against breakage, and initial cracking at the weakest point of the composite as the connecting point between AC and the polymer [24]. Impact strength decreased with increase in ADC content, significantly lower than neat LDPE. The composite foams containing 1-7 wt% of ADC at 5 wt% AC dosage exhibited reduction of

impact strength at approximately 50-70% and 70-80%, compared with the non-foamed composite and LDPE resin respectively. Nitrogen and carbon monoxide were generated from ADC during the foaming process, leading to bubble growth which prevented proper bonding between the polymer and AC, resulting in the development and propagation of cracks. This cracking behavior was also in good agreement with research conducted by Matuana and Mengeloglu [25]. The impact strength of composite foams having 0-20 wt% of AC at 7 wt% ADC content was in the range of 0.34-0.77 J mm^{-1}, much lower than that of pure LDPE (5.60 J mm^{-1}). The impact resistance distinctly reduced with the addition of ACs, especially at high AC concentration e.g. 20 wt% due to the presence of AC agglomerations in the polymer matrix, corresponding to SEM micrographs. The AC aggregates increased the number of cracks at the stress concentration points, and required less energy to elongate the crack propagation [26, 27]. Moreover, some AC particles in the composite foams separated from the polymer matrix because of a lack of good adhesion between the polymer and ACs with bubbles increasing the distance between them.

3.5 Thermal properties

Thermal stability is very important for polymeric materials as it is often the limiting factor both in processing and in end-use applications. Table 2 presents the T_c, T_m, T_d and X_c at various ADC and AC concentrations. The T_c and T_m of the composite foams remained almost constant with the addition of ADC and AC at 91-94^oC and 113-116^oC respectively, compared with LDPE resin (T_c = 92^oC and T_m = 115^oC). At constant AC loading (5 wt%), the T_d increased to 498^oC at 0 wt% of ADC, and then decreased to 473^oC at 1 wt% of ADC, compared with LDPE resin (T_d = 487^oC). The T_d of the composite foams altered slightly to 477-479^oC with ADC dosages of 3, 5 and 7 wt%. The addition of ADC in the composite foam increased the porosity, causing high heat accumulation inside and therefore decomposition occurred at lower temperature. At the same ADC content (7 wt%), the addition of AC at 5 wt% of resin

decreased the thermal stability by around 8°C compared with neat LDPE and LDPE foam without AC loading. This result showed that the porous structure of the composite foam had more effect than the presence of AC particles at low concentration, since the addition of a particulate phase in the polymeric matrix was accompanied by an increment in thermal stability of the corresponding polymer [3]. The T_d of composite foams increased when the AC content was higher than 5 wt% of resin and remained constant at 490°C. The improvement in the resistance to thermal degradation of polymeric foam due to the presence of AC particles could be attributed to the hindered diffusion of volatile decomposition products within the composite foams, and it was strongly dependent on the AC-polymer chain interactions [28]. As the amount of AC increased, more AC aggregates were produced, leading to the reduction of LDPE-AC interaction which resulted in no increment of thermal stability improvement. The X_c changed slightly from 38 to 42% with increasing ADC content at fixed AC concentration (5 wt%), compared to LDPE resin (40%). However, the X_c of the composite foam decreased markedly to 36% at 7 wt% of ADC loading. In addition, the X_c decreased from 40 to 31% with increasing AC content from 0 to 20 wt% at constant ADC dosage (7 wt%). At high ADC and AC dosages, the proportion of LDPE in the composite foam was reduced, resulting in low crystallization phenomena.

4. CONCLUSIONS

LDPE-AC composite foams containing different ADC and AC loadings were prepared using an extrusion method. The composite foams possessed closed cell structure with average pore diameter in the range of 3-150 μm. The density of the composite foams decreased but the void fraction increased as the content of ADC increased due to higher gas liberation. Moreover, the largest cell size was observed in composite foams containing higher amounts of ADC. At low AC dosages, the density of the composite foams decreased with increasing void fraction compared to composite foam without AC, because more foaming nucleation centers were induced

by adding AC into the composite foam leading to the generation of more gas bubble coalescence. However, the addition of AC up to 15-20 wt% decreased the cell formation, and the average cell size decreased with increasing AC content due to AC agglomeration which reduced the cell growth and produced cells with smaller dimensions. The maximum reduction of density by 30% with a void fraction of 30% was achieved when ADC and AC were applied at 7 wt% and 10 wt% respectively. Larger amounts of ADC and AC led to LDPE-AC composite foams with lower tensile and impact strength, as a result of the formation of cellular structure, AC agglomeration, and the reduction of polymer matrix. The T_c and T_m changed insignificantly as the ADC and AC concentrations increased. The T_d tended to decrease when the ADC loading increased, since more porosity was created causing high heat accumulation inside. On the contrary, increase in AC concentration had a tendency to enhance the T_d of the composite foams. The X_c of composite foams reduced slightly with increasing ADC content. As the degree of AC loading increased, the X_c significantly decreased. At high ADC and AC contents, the proportion of LDPE in the composite foam reduced, resulting in low crystallization phenomena.

ACKNOWLEDGEMENTS

The authors would like to acknowledge the National Metal and Materials Technology Center (MTEC) under the National Science and Technology Development Agency (NSTDA), Thailand for financial support, sample preparation, and characterization.

REFERENCES

[1] Park C.P., Polyolefin Foam; in Klempner D. and Sendijarevic V., eds., *Handbook of Polymeric Foams and Foam Technology*, Hanser Publishers, Munich, 2004: 233-299.

[2] Ameli A., Nofar M., Jahani D., Rizvi G. and Park C.B., Development of high void fraction polylactide composite foams using injection molding: Crystallization and foaming behaviors, *Chem. Eng. J.*, 2015; **262:** 78-87.

[3] Zhai W., Park C.B. and Kontopoulou M., Nanosilica addition dramatically improves the cell morphology and expansion ratio of polypropylene heterophasic copolymer foams blown in continuous extrusion, *Ind. Eng. Chem. Res.*, 2011; **50:** 7282-7289.

[4] Lee L.J., Zeng C., Cao X., Han X., Shen J. and Xu G., Polymer nanocomposite foams, *Compos. Sci. Technol.*, 2005; **65:** 2344-2636.

[5] Saiz-Arroyo C., Saja J.A.D., Velasco J.I. and Rodríguez-Pérez M.A., Moulded polypropylene foams produced using chemical or physical blowing agents: Structure-properties relationship, *J. Mater. Sci.*, 2012; **47:** 5680-5692.

[6] Bledzki A.K. and Faruk O., Injection moulded microcellular wood fibre-polypropylene composites, *Compos. Part A-Appl. Sci. Manuf.*, 2006; **37:** 1358-1367.

[7] Petchwattana N. and Covavisaruch S., Influences of particle sizes and contents of chemical blowing agents on foaming wood plastic composites prepared from poly (vinyl chloride) and rice hull, *Mater. Design*, 2011; **32:** 2844-2850.

[8] Zhou J., Zhengjun Y., Zhou C., Wei D. and Li S., Mechanical properties of PLA/PBS foamed composites reinforced by organophilic montmorillonite, *J. Appl. Polym. Sci.*, 2014; doi:10.1002/APP.40773.

[9] Matuana L.M., Park C.B. and Balatinecz J.J., Cell morphology and property relationships of microcellular foamed PVC/wood-fiber composites, *Polym. Eng. Sci.*, 1998; **37:** 1862-1872.

[10] Matuana L.M., Park C.B. and Balatinecz J.J., Structures and mechanical properties of microcellular foamed polyvinyl chloride, *Cell. Polym.*, 1998; **17:** 1-16.

[11] Ibeh C.C. and Lee S.W., Current trends in nanocomposite foams, *J. Cell. Plast.*, 2008; **44:** 498-515.

[12] Shen J., Zeng C. and Lee L.J., Synthesis of polystyrene-carbon nanofibers nanocomposite foams, *Polymer*, 2005; **46:** 5218-5224.

[13] Chen L., Schadler L.S. and Ozisik R., An experimental and theoretical investigation of the compressive properties of multi-walled carbon nanotube/poly (methyl methacrylate) nanocomposite foams, *Polymer*, 2011; **52:** 2899-2909.

[14] Singh C.K., Sahu J.N., Mahalik K.K., Mohanty C.R., Mohan B.R. and Meikap B.C., Studies on the removal of Pb (II) from wastewater by activated carbon developed from Tamarind wood activated with sulphuric acid, *J. Hazard. Mater.*, 2008; **153:** 221-228.

[15] Hesas R.H., Arami-Niya, A., Daud W.M.A.W. and Sahu J.N., Preparation and characterization of activated carbon from apple waste by microwave-assisted phosphoric acid activation: Application in methylene blue adsorption, *Bioresources*, 2013; **8:** 2950-2966.

[16] Crini G., Non-conventional low-cost adsorbents for dye removal: a review, *Bioresour. Technol*., 2006; **97:** 1061-1085.

[17] Pinto J., Rodríguez-Pérez M.A. and Saja, J.A.D., XI Reunion del Grupo Especializado de Polímeros (GEP) 10-24 September 2009, Valladolid-Spain 2009.

[18] Zakaria Z., Ariff Z.M. and Sipaut C.S., Effects of parameter changes on the structure and properties of low-density polyethylene foam, *J. Vinyl. Addit. Technol.*, 2009; **15:** 120-128.

[19] Babaei I., Madanipour M., Farsi M. and Farajpoor A., Physical and mechanical properties of foamed HDPE/wheat straw flour/nanoclay hybrid composite, *Compos. Part B-Eng.*, 2014; **56:** 163-170.

[20] Lee Y., Sain M., Kuboki T. and Park C., Extrusion foaming of nano-clay-filled wood fiber composites for automotive applications, *SAE Int. J. Mater. Manf.*, 2009; **1:** 641-647.

[21] Faruk O., Bledzki A.K. and Matuana L.M., Microcellular foamed wood-plastic composites by different processes: a review, *Macromol. Mater. Eng.*, 2007; **292:** 113-127.

[22] Blair E.A., ASTM special publication, *Resinography. Cell. Plast.*, 1967; **414**: 84.

[23] Ashori A. and Nourbakhsh A., Effects of nanoclay as a reinforcement filler on the physical and mechanical properties of wood based composite, *Compos. Mater.*, 2009; **43:** 1869-1875.

[24] Kordkheili H.Y., Farsi M. and Rezazadeh Z., Physical, mechanical and morphological properties of polymer composites, *Compos. Part B-Eng.*, 2013; **44:** 750-755.

[25] Mengeloglu F. and Matuana L.M., Mechanical properties of extrusion-foamed rigid PVC/wood-flour composites, *J. Vinyl. Addit. Technol.*, 2003; **9:** 26-31.

[26] Liany Y., Tabei A., Farsi M. and Madanipour M., effect of nanoclay and magnesium hydroxide on some properties of HDPE/wheat straw composites, *Fiber. Polym.*, 2013; **14:** 304-310.

[27] Park S.H. and Bandaru P.R., Improved mechanical properties of carbon nanotube/polymer composites through the use of carboxyl-epoxide functional group linkages, *Polymer*, 2010; **51:** 5071-5077.

[28] El Achaby M., Arrakhiz F.E., Vaudreuil S., El Kacem Q.A., Bousmina M. and Fassi-Fehri O., Mechanical, thermal, and rheological properties of graphene-based polypropylene nanocomposites prepared by melt mixing, *Polym. Composite.*, 2012; **33:** 733-744.

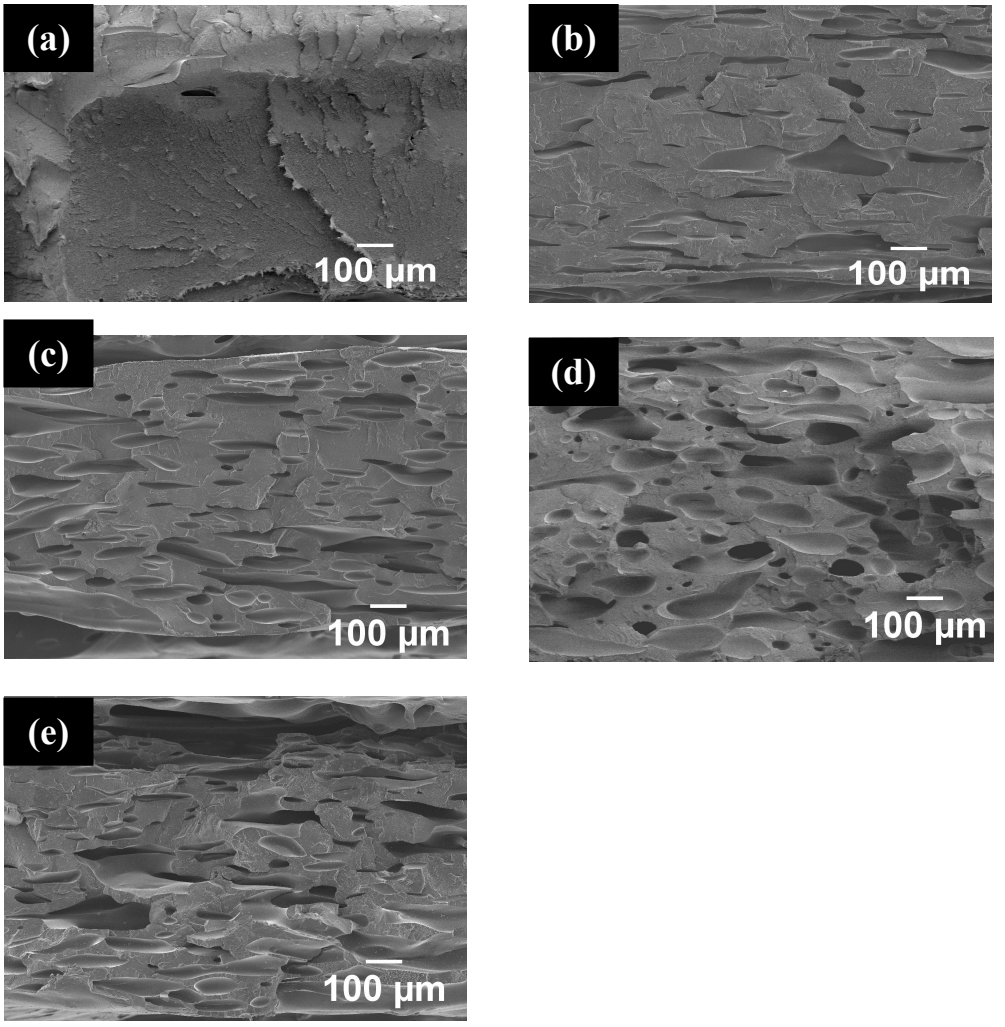

Figure 1. SEM micrographs of foamed composites with various ADC contents (wt%) at 5 wt% of AC: (a) 0, (b) 1, (c) 3, (d) 5, and (e) 7.

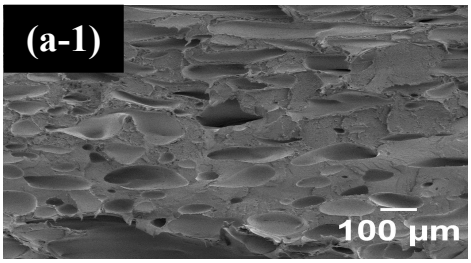
(a-1)
100 μm

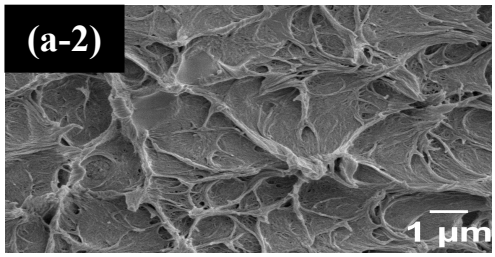
(a-2)
1 μm

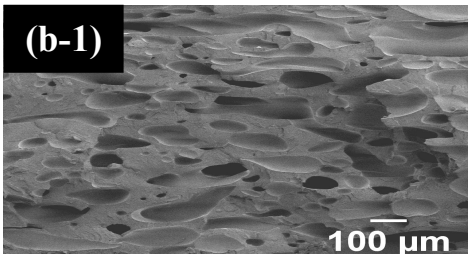
(b-1)
100 μm

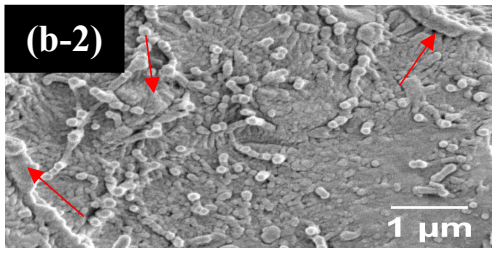
(b-2)
1 μm

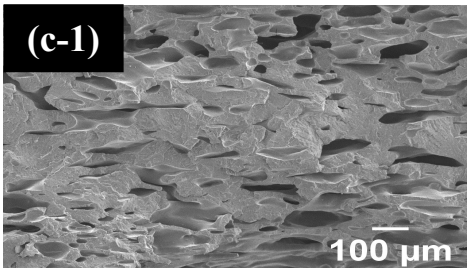
(c-1)
100 μm

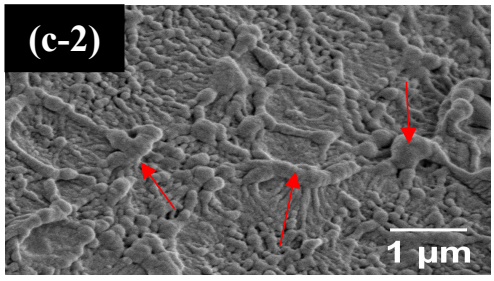
(c-2)
1 μm

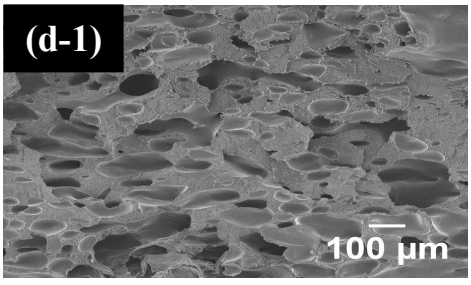
(d-1)
100 μm

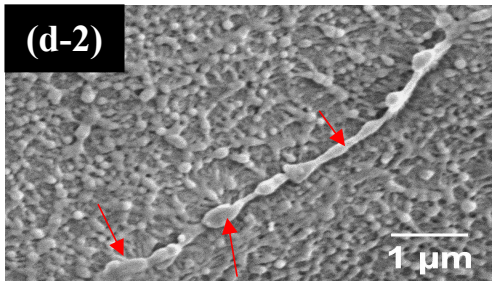
(d-2)
1 μm

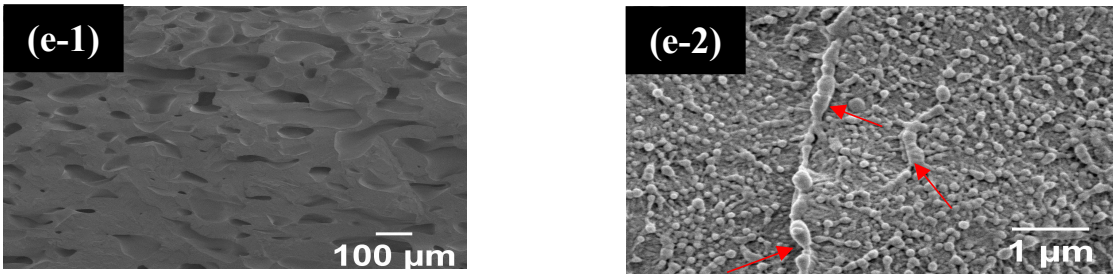

Figure 2. SEM micrographs of foamed composites with various AC contents (wt%) at 7 wt% of ADC content: (a-1)-(a-2) 0, (b-1)-(b-2) 5, (c-1)-(c-2) 10, (d-1)-(d-2) 15, and (e-1)-(e-2) 20.

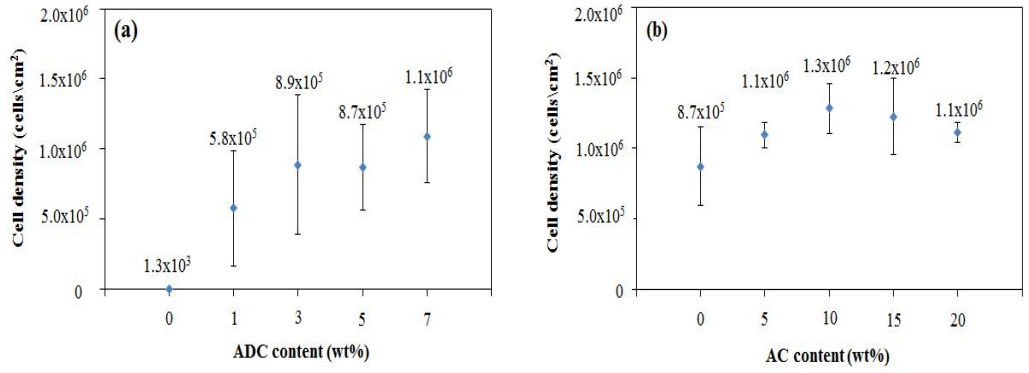

Figure 3. Cell density of LDPE-AC composite foams (a) at various ADC contents (5.0 wt% of AC loading) and (b) at different AC contents (7 wt% of ADC loading).

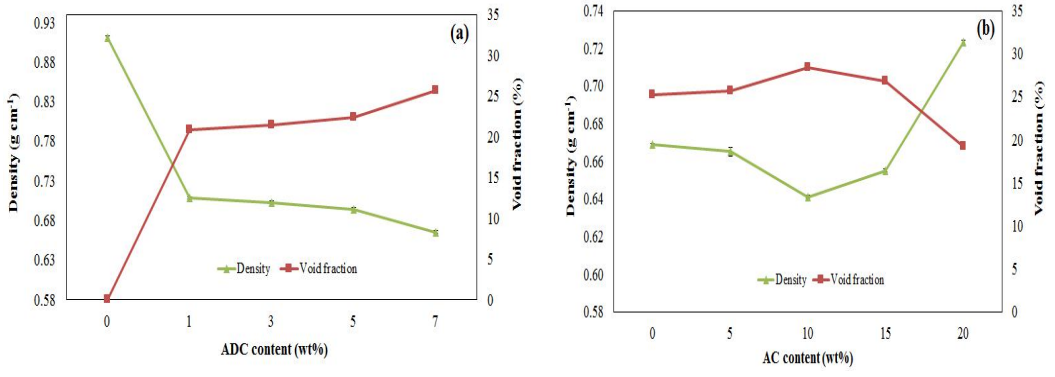

Figure 4. Density and void fraction of LDPE-AC composite foams with (a) at various ADC contents (5 wt% of AC loading) and (b) at different AC contents (7 wt% of ADC loading).

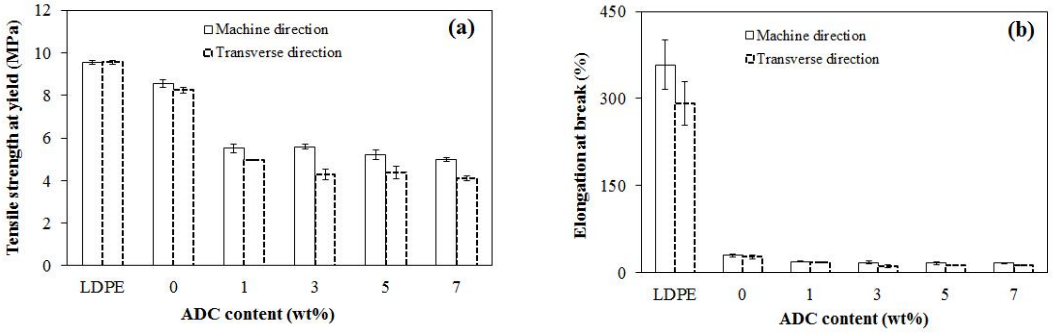

Figure 5. Tensile properties of LDPE and composite foams with various ADC contents at 5 wt% of AC loading: (a) tensile strength at yield and (b) elongation at break.

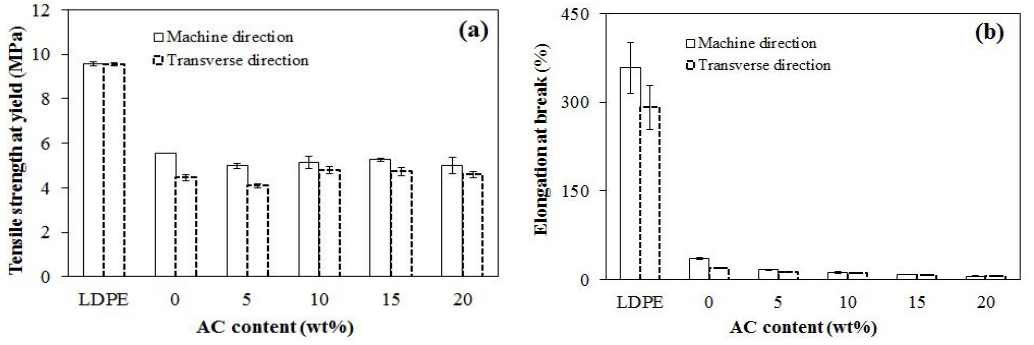

Figure 6. Tensile properties of LDPE and composite foams with various AC contents at 7 wt% of ADC loading: (a) tensile strength at yield and (b) elongation at break.

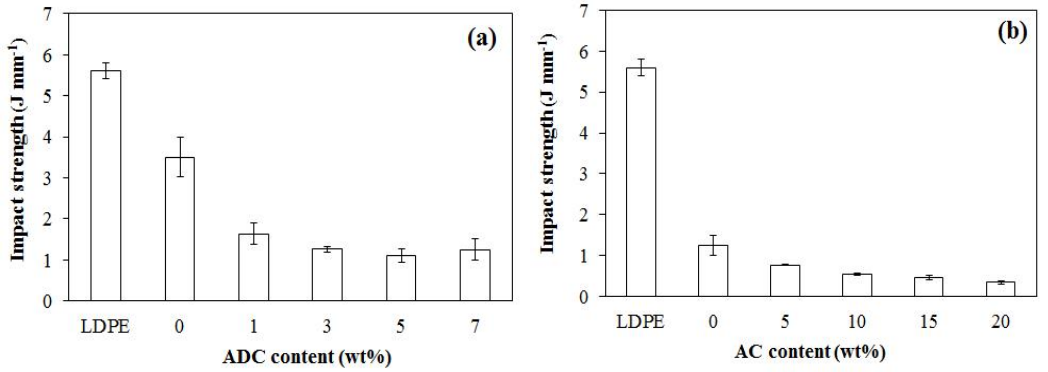

Figure 7. Impact strength of LDPE and composite foams (a) at various ADC contents (5 wt% of AC loading) and (b) at different AC contents (7 wt% of ADC loading).

Table 1. The composition of LDPE-AC composite foams.

Sample	ADC (wt%)	AC (wt%)	ZnO (wt%)	Annox20 (wt%)
0ADC-5AC	0.0	5.0	1.0	0.2
1ADC-5AC	1.0	5.0	1.0	0.2
3ADC-5AC	3.0	5.0	1.0	0.2
5ADC-5AC	5.0	5.0	1.0	0.2
7ADC-5AC	7.0	5.0	1.0	0.2
7ADC-0AC	7.0	0.0	1.0	0.2
7ADC-10AC	7.0	10.0	1.0	0.2
7ADC-15AC	7.0	15.0	1.0	0.2
7ADC-20AC	7.0	20.0	1.0	0.2

Table 2. Thermal properties of LDPE-AC composite foams.

Sample	T_c (°C)	T_m (°C)	T_d (°C)	X_c (%)
LDPE	92	115	487	40
0ADC-5AC	93	114	498	40
1ADC-5AC	92	116	473	42
3ADC-5AC	91	116	479	40
5ADC-5AC	94	113	477	38
7ADC-5AC	92	115	479	36
7ADC-0AC	92	115	487	40
7ADC-10AC	92	115	490	34
7ADC-15AC	93	115	490	31
7ADC-20AC	93	115	490	31